Outline:

1.- Introduction

2.- Brief description of ALBA phase I beamlines: Xaloc, Mistral, Boreas and Circe PEEM branch including examples

3.- Phase II beamlines : MIRAS (IR beamline) and LOREA (Angle resolved photoemission)

4.- Examples of applications of two possible phase III beamlines: micro-XAS and hard X ray imaging

Characteristics of synchrotron radiation

- High intensity, allowing the study of very small samples, surfaces, or fast phenomena

- Ability to be strongly focused providing access to characterization across a wide range of length scales from centimeter to nanometer

- Sensitivity to chemical elements and their speciation

- Ability to follow a process in real time

- Ability to work in situ with real-life samples such as batteries, catalysis, solidification of alloys or transport of liquids in porous materials.

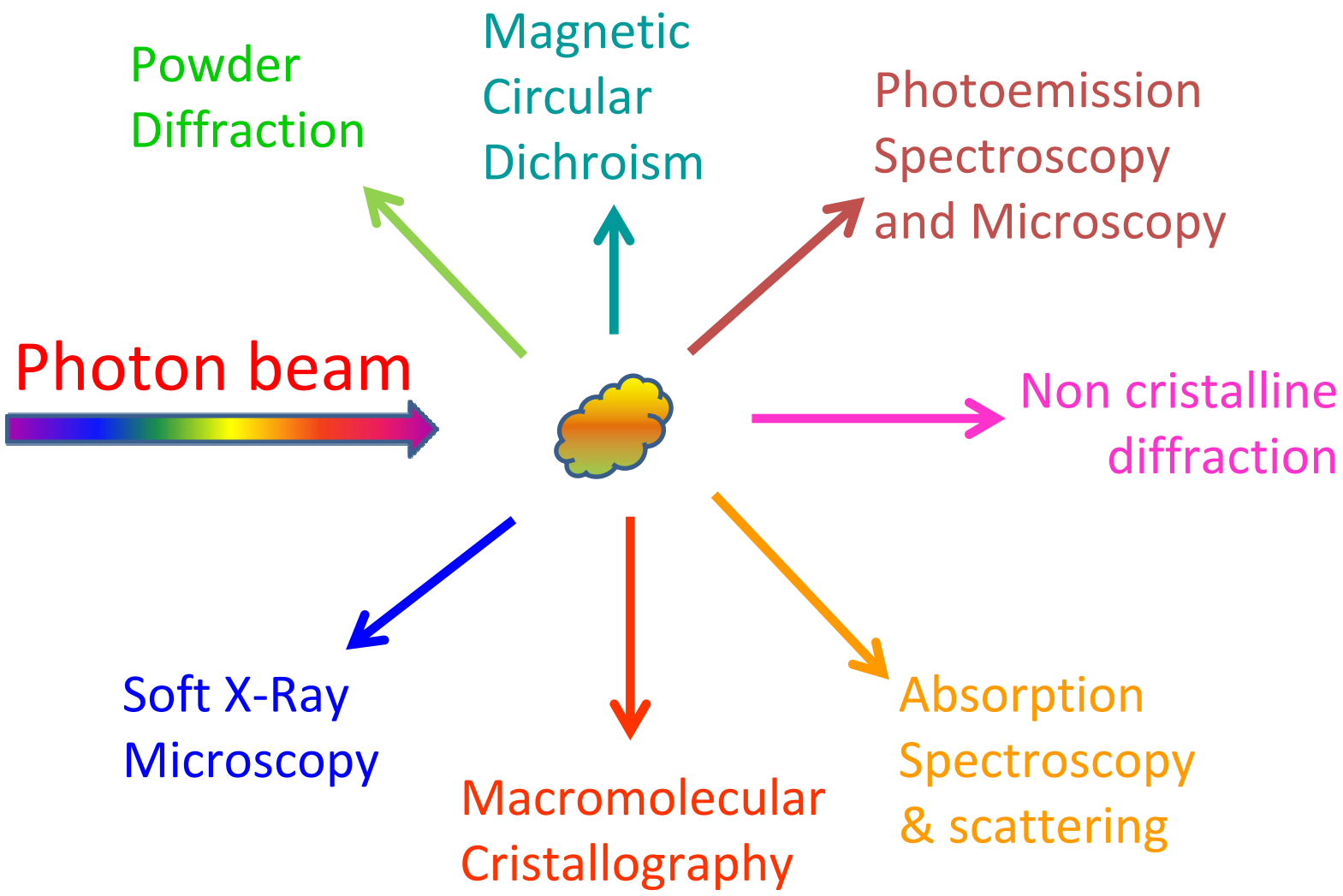
Powder
Diffraction
Magnetic
Circular
Dichroism
Photoemission
Spectroscopy
and Microscopy
Photon beam
Non cristalline
diffraction
Soft X-Ray
Microscopy
Macromolecular
Cristallography
Absorption
Spectroscopy
& scattering

SEVEN BEAMLINES

BL24 - CIRCE

Photoemission Spectroscopy and Microscopy

ES1: PEEM **ES2: NAPP**

BL29 - BOREAS

Beamline for
Resonant Absorption and Scatteri

ES1: HECTOR **ES2: MARES**

BL09 - MISTRAL

Soft X-ray microscope beamline

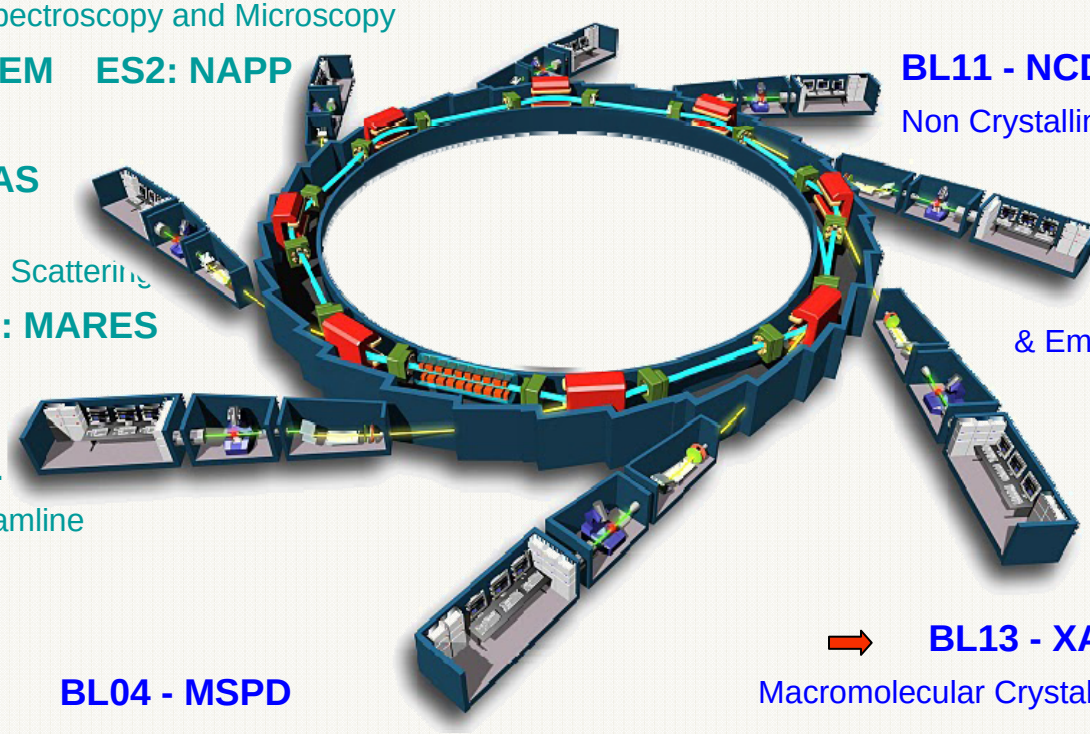

BL11 - NCD

Non Crystalline Diffraction

BL22 - CLAESS

Core Level Absorption
& Emission Spectroscopy Beamline

BL13 - XALOC

Macromolecular Crystallography beamline

BL04 - MSPD

Materials Science and Powder Diffraction Beam Line

ES1: HRPD **ES2: High Pressure**

Macromolecular Crystallography

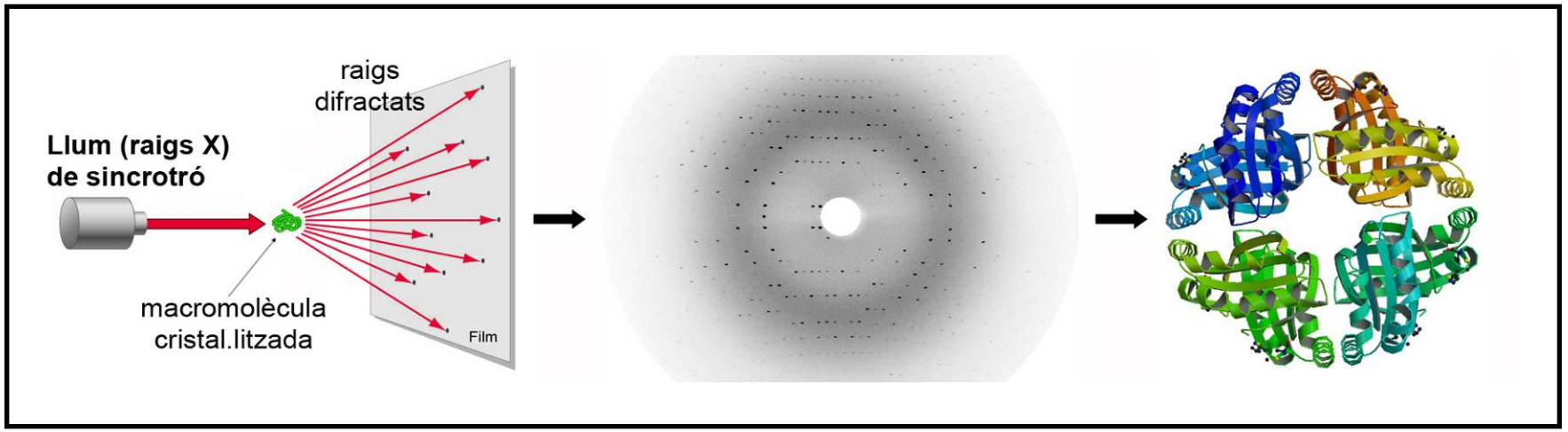

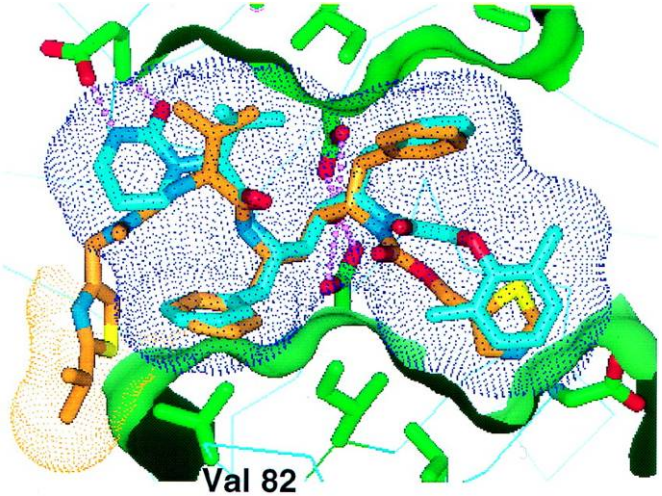

HIV proteasa

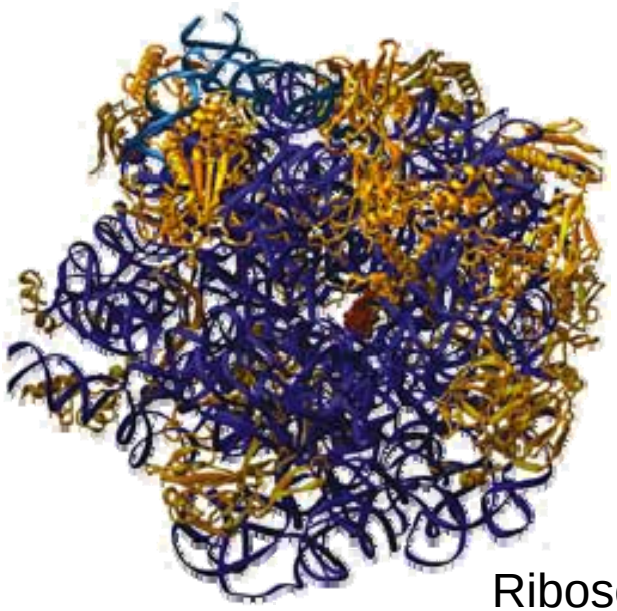

Ribosoma

Sham *et al.* ANTIMICROBIAL AGENTS AND CHEMOTHERAPY (1998)

BL13 XALOC – Macromolecular Crystallography

Photon source (IVU-21) : in-vacuum undulator, 92 poles, period of 21.6 mm, with a gap variable, L = 2.1 m between 5.5 - 30 mm, Beff: 0.8 T

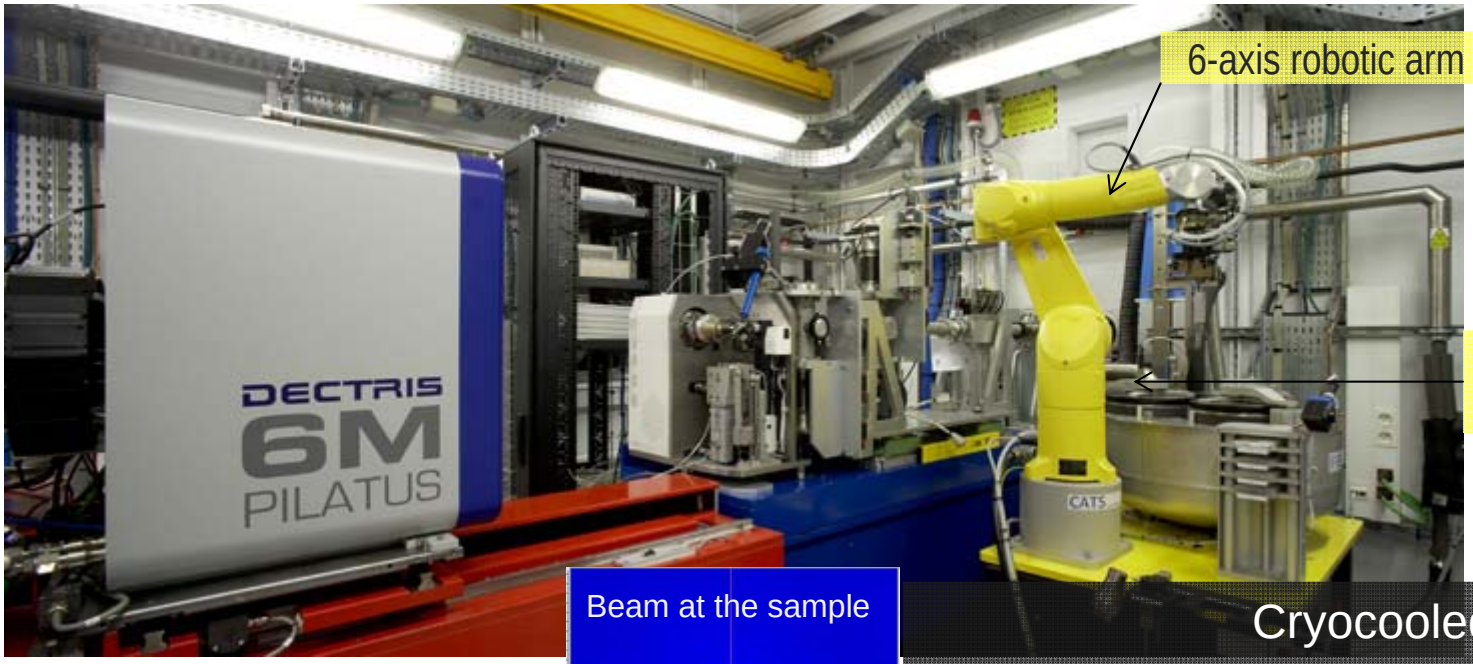

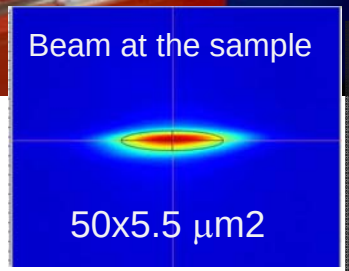

Cryocooled monochromator
KB mirror pair
End station : Goniometer , automatic sample changer

- ***Flexible and reliable for solving structures of macromolecules and complexes.***
- ***Copes with a broad variety of crystal sizes and unit cell parameters.***
- ***Allows both wavelength dependent and independent experiments.***
- ***Photon energy range: 5 to 22 keV.***

CRYSTAL GROWTH & DESIGN

Article

pubs.acs.org/crystal

Design, Synthesis, and Structural Analysis of Turn Modified *cyclo*-$(\alpha\beta^3\alpha\beta^2\alpha)_2$ Peptide Derivatives toward Crystalline Hexagon-Shaped Cationic Nanochannel Assemblies

José M. Otero,[†,§] Matthijs van der Knaap,[†] Antonio L. Llamas-Saiz,[‡] Mark J. van Raaij,[δ] Manuel Amorín,[φ] Juan R. Granja,[φ] Dmitri V. Filippov,[†] Gijsbert A. van der Marel,[†] Herman S. Overkleeft,[†] and Mark Overhand*[,†]

ABSTRACT: Intrigued by the not fully extended hairpin monomeric structure of the previously reported *cyclo*-$(\alpha\beta^3\alpha\beta^2\alpha)_2$ peptide **2**, as well as its nanochannel crystallographic assembly, we here investigate the structural properties of a series of turn derivatives (**3**–**17**). Five crystallographic monomeric structures of the symmetric and asymmetric *cyclo*-$(\alpha\beta^3\alpha\beta^2\alpha)_2$ peptides **3**–**17** are found; the novel saddlelike (**4** and **16**) and the twisted hairpin (**6**) conformers, as well as the not fully extended hairpins **7** and **14**. The pentafluorophenyl/1-naphthyl and pentafluorophenyl/9-phenanthryl derivatives **7** and **14**, respectively, adopt the anticipated hexagon-shaped crystalline nanotube assemblies, resembling the crystal packing of the parent peptide **2**. The structural analysis of the compounds as described here can serve as a basis for biological applications, such as the design of β-sheet mimics or for the development of functional nanomaterials.

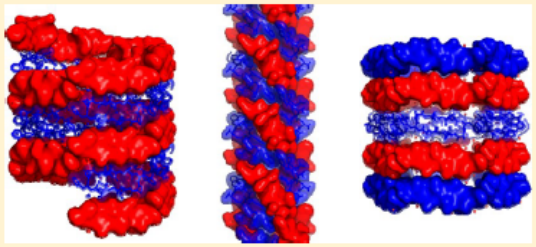

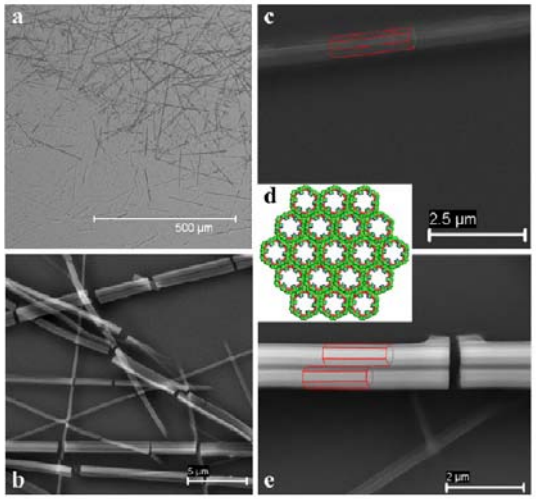

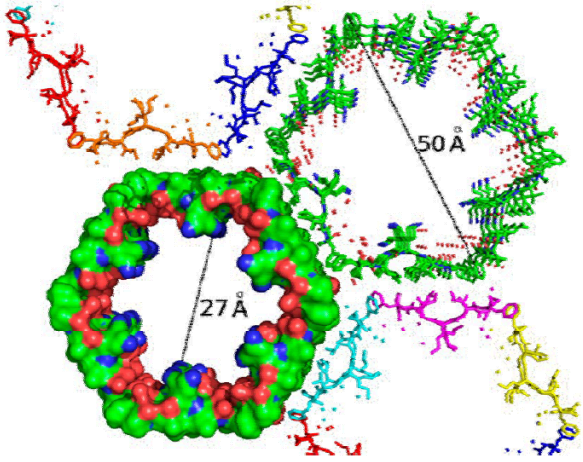

El microscopio de rayos X de Alba

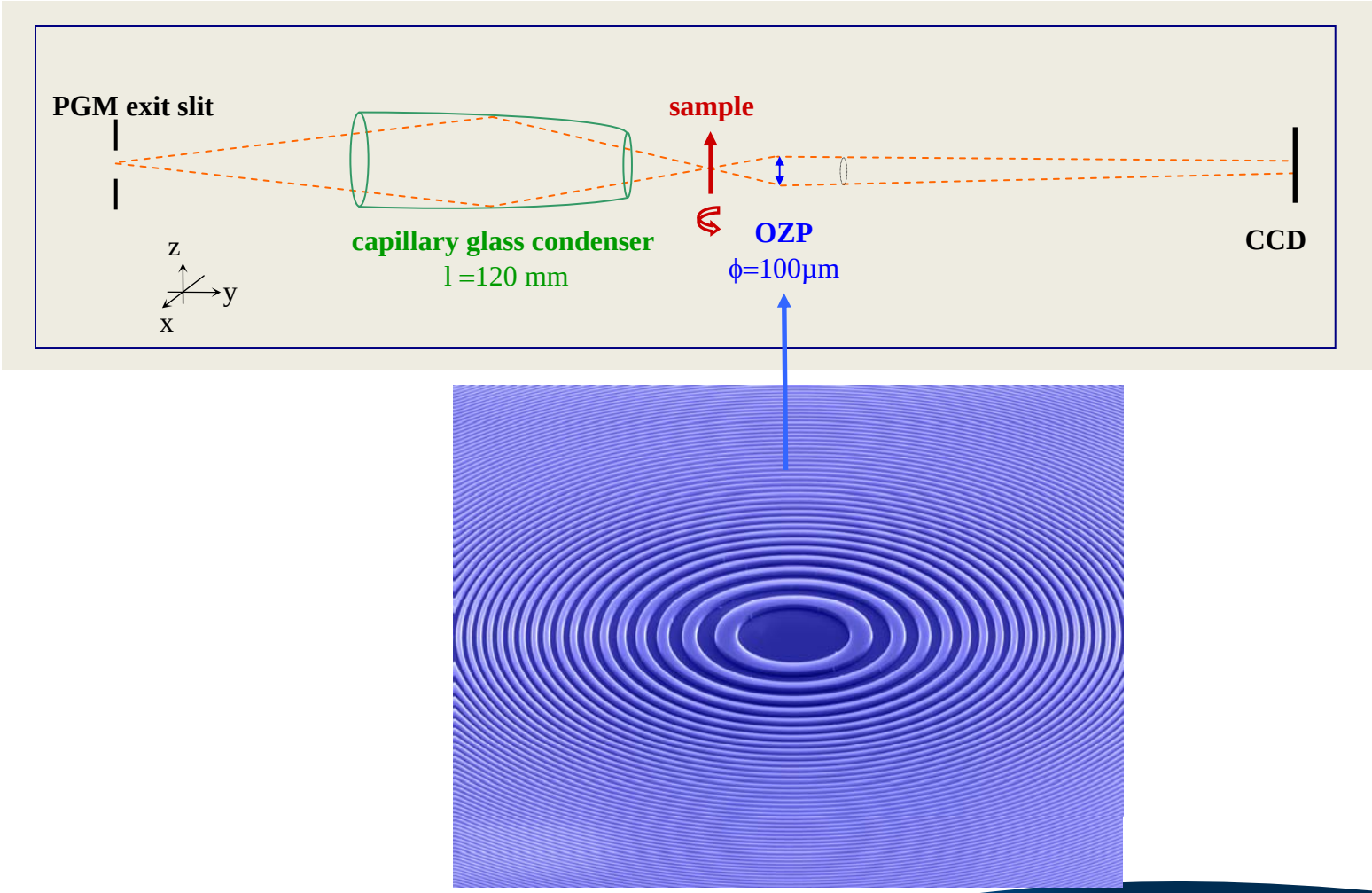

BL09 Mistral - Transmission Soft X-Ray Microscopy

Photon source: dipole
ρ = 7.6 m

Only two other similar Microscopes in the world: BESSY-II and ALS

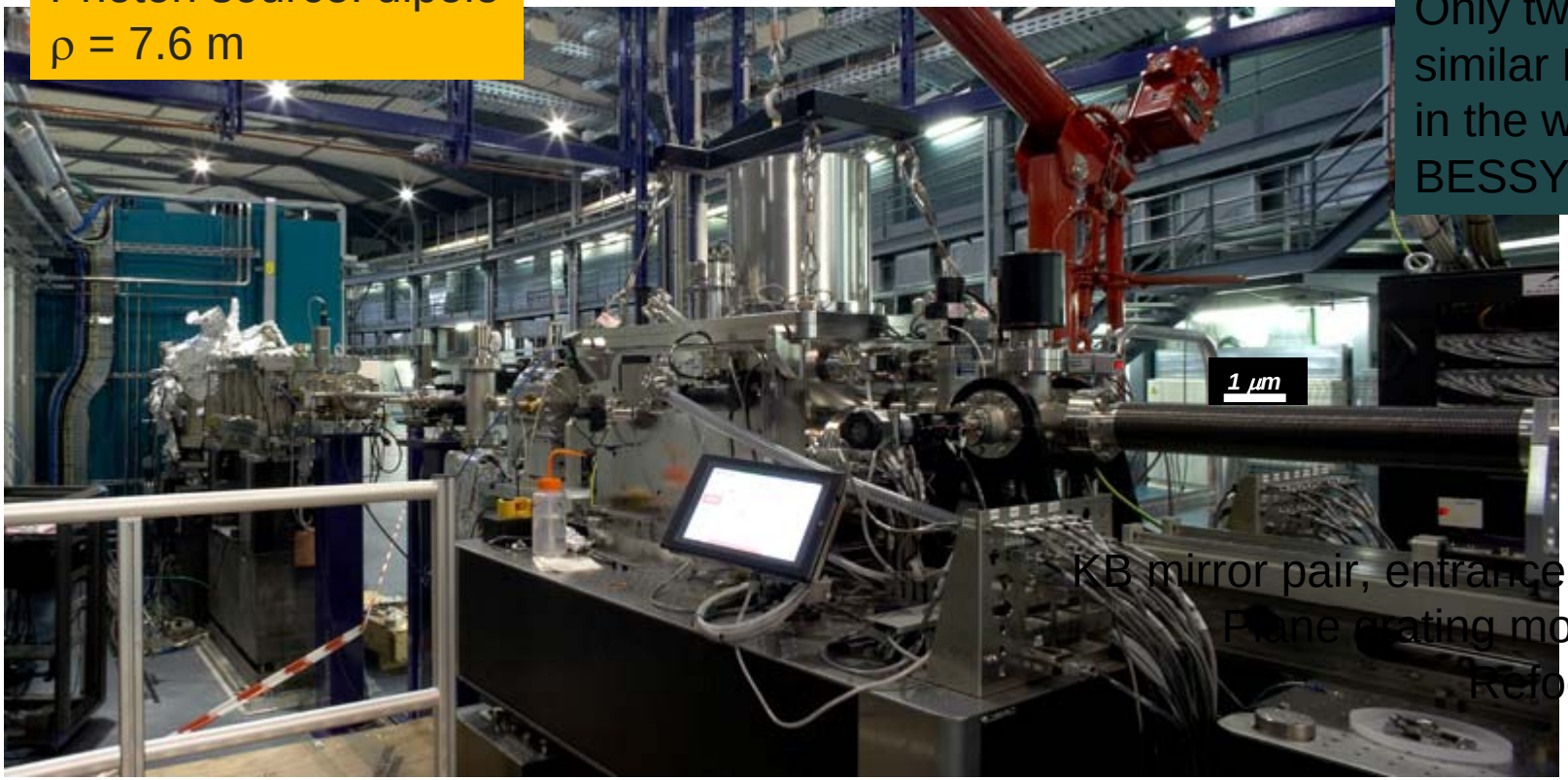

KB mirror pair, entrance and exit slits
Plane grating monochromator
Refocusing mirror
Microscope

- Cryo nano-tomography in water window and multi-keV spectral regions for biological applications.
- Spectroscopic imaging.
- Present photon energy range: 270 to 1200 eV, upgradable to 2600 eV in the future.
- 30 nm 2D resolution

SXT: sub-cellular organelles

N: nucleus
NM: nuclear membrane
ER: endoplasmic reticulum
G: golgi
n: nucleoli
M: mitochondrion
LV: lipid vesicle

Huh- 7.5 cells (human cell line)

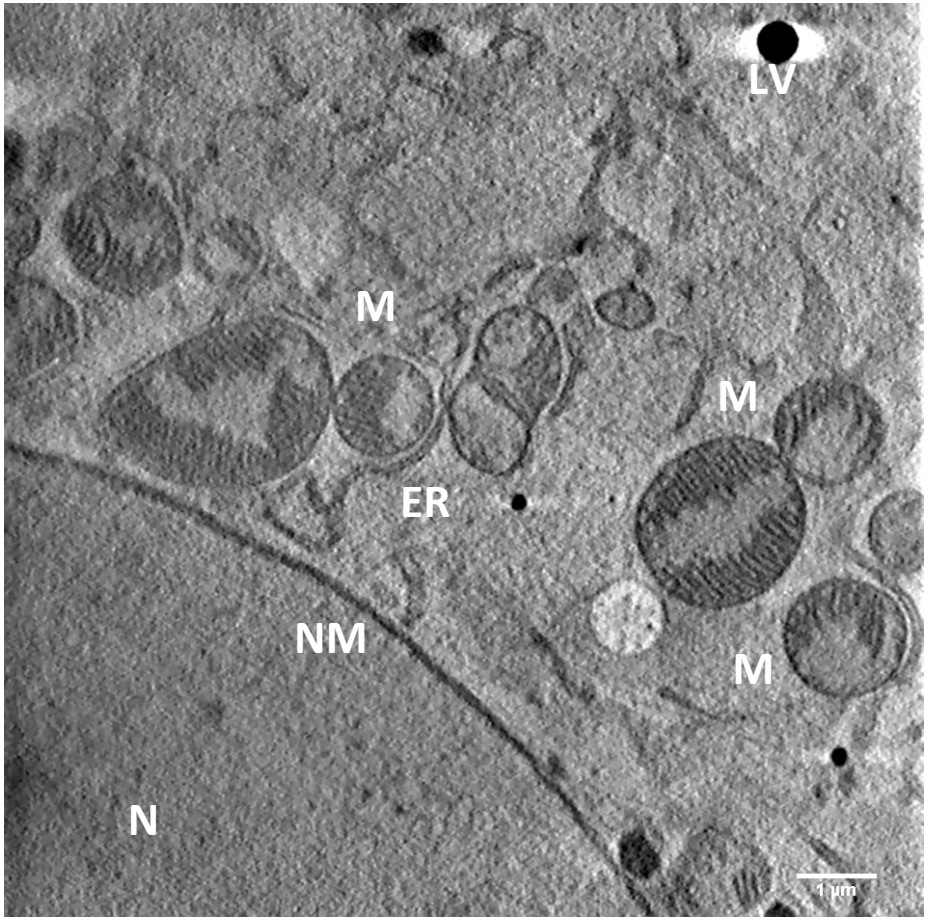

Mitochondria

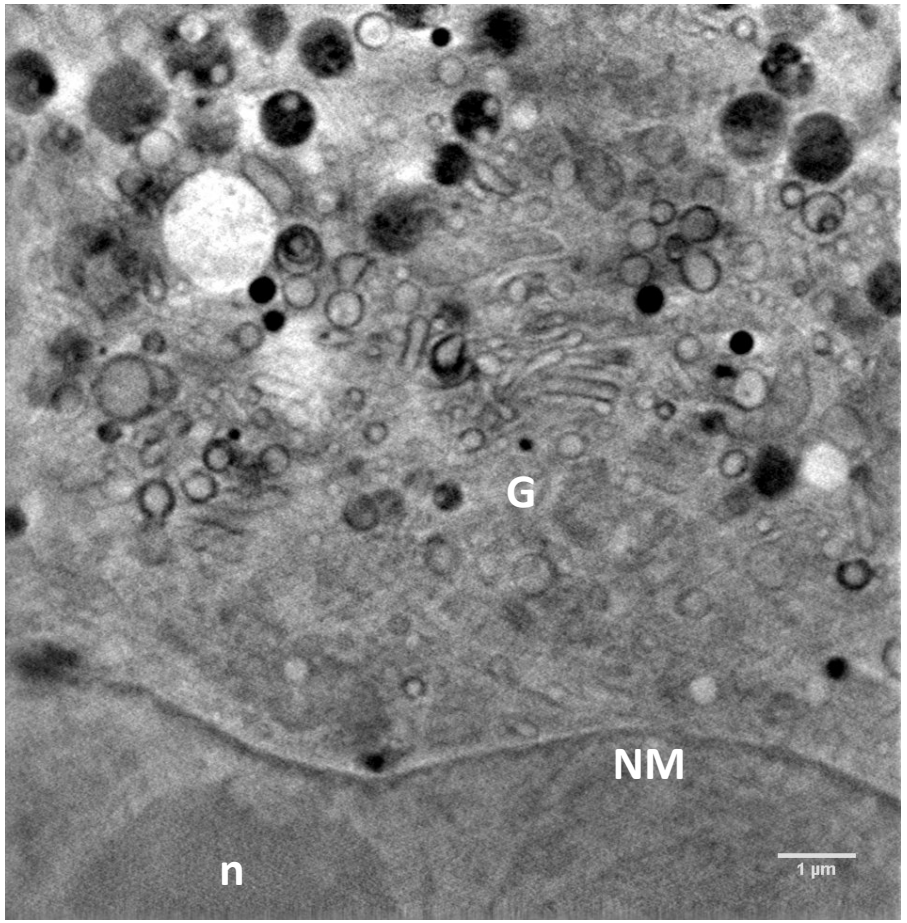

Golgi

"Boreas running", (460 b.c., Yale Univ.)

BOREAS, Beamline Of REsonant Absorption and Scattering

X ray absorption spectroscopy:

Absorption of X rays occurs at well defined energies characteristic of the absorbing atoms

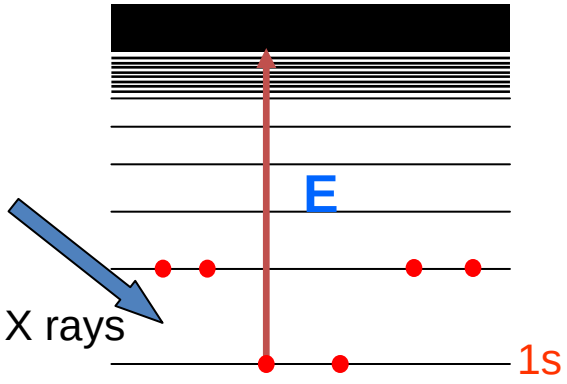

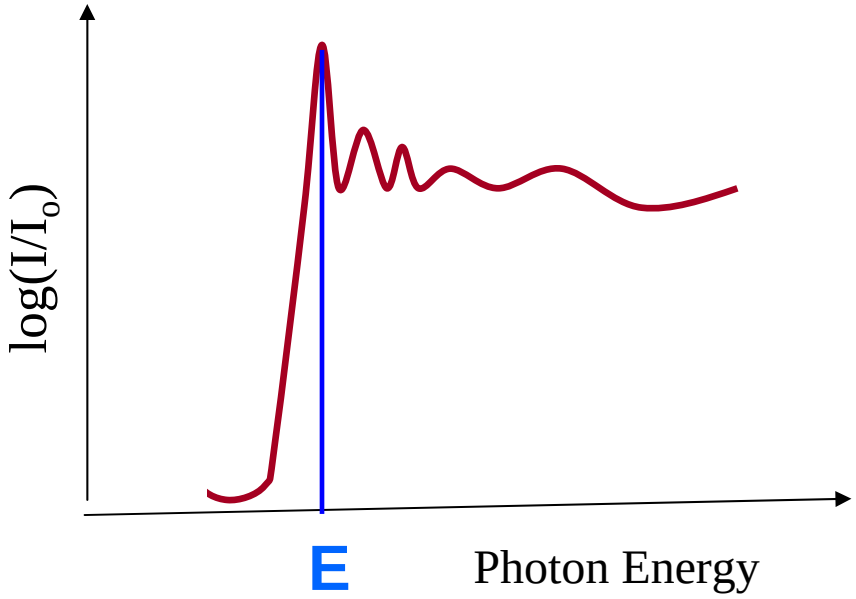

BOREAS, Beamline Of REsonant Absorption and Scattering

Soft x-rays: 80-4000 eV, variable polarization
two endstations: XAS, XMCD (7 T magnet) and Soft X ray Reflectivity

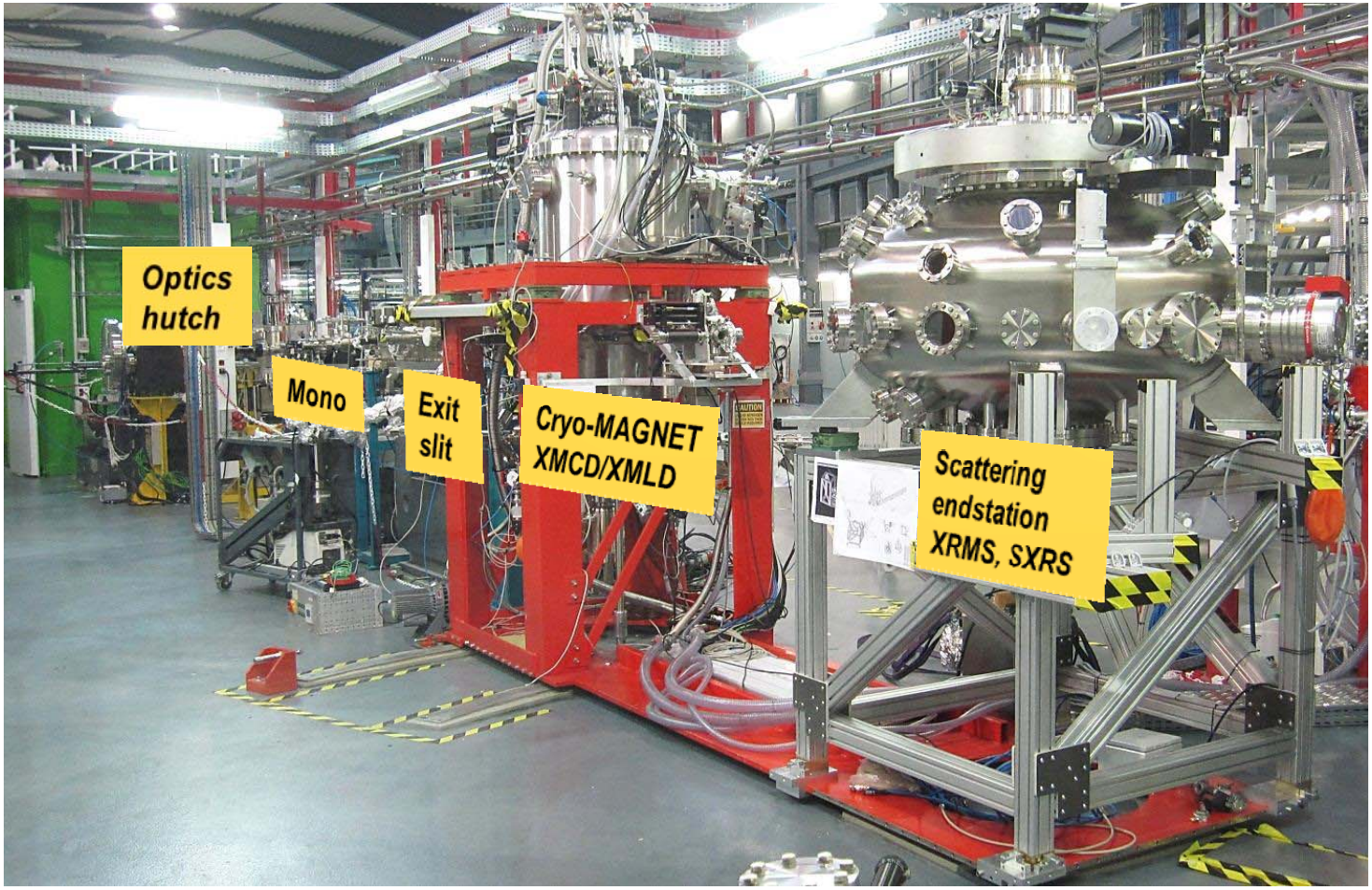

Aplicacion al estudio de ferritas

(Tesis doctoral Eduardo Soriano , UAB Sep, 2013)

Motivacion: Para mejorar las propiedades de transporte de superconductores YBaCuO y controlar sus defectos estructurales que deterioran su rendimiento electrico, se introducen nanoparticulas de ferrita MnFeO a fin de estabilizar y bloquear los vortices superconductores.

Las nanoparticulas se sintetizan o bien con metodos que contienen tratamientos termicos o con metodos asistidos con micro-ondas. Se quiere estudiar si la sintesis y el proceso de introduccion de las nanoparticulas afecta a su estructura electronica. Para ello se utiliza XMCD en Boreas.

Absorption of X rays of different energies near the Mn L3 edge

Free nanoparticles

Mn

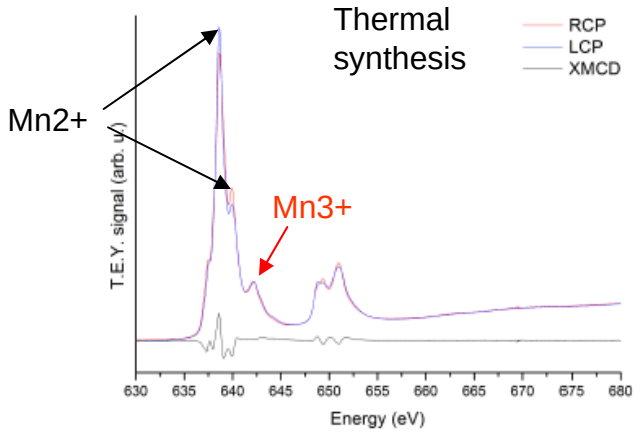

(a) $MnFe_2O_4$-T Mn edge

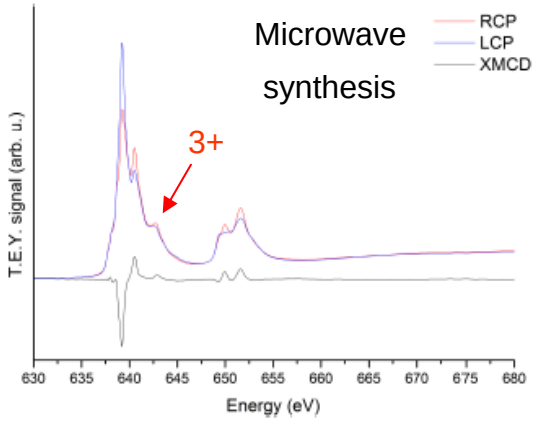

(c) $MnFe_2O_4$-MW Mn edge

Nanoparticles in YBaCuO

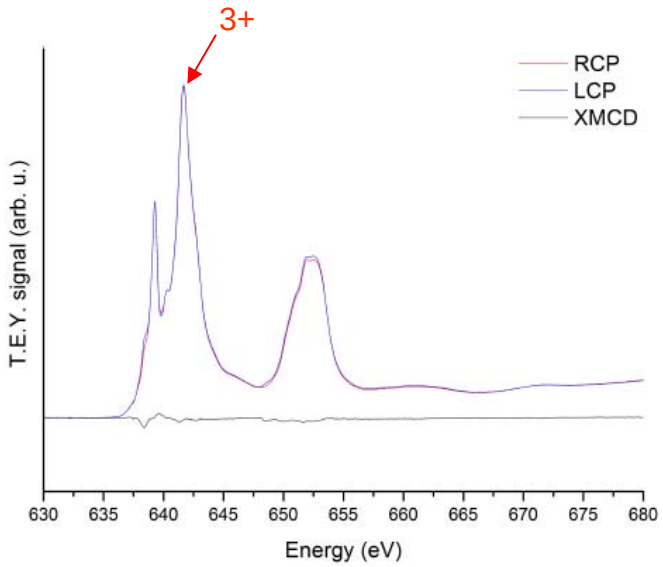

The NP inside the superconductor have different proportions of oxidation states and the Mn atoms are more oxidized

This is mostly at the surface region

Electrons have spin  . The sum of the spin of all the electrons of an atom is in most cases equal to zero, but in some cases no : Fe , Co , Ni. The non zero spin makes the atoms magnetic

X ray of specific energy

X ray spin

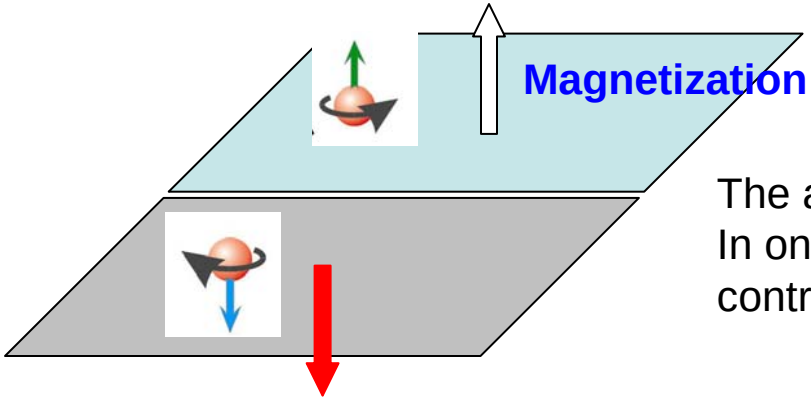

The absorption of X rays is different In one side than the other: magnetic contrast

Boreas BL29 – Recent Scientific Highlights

Nanoscale

RSC Publishing

PAPER

View Article Online
View Journal | View Issue

Direct observation of rotatable uncompensated spins in the exchange bias system Co/CoO–MgO

Cite this: *Nanoscale*, 2013, **5**, 10236

Chuannan Ge,[ab] Xiangang Wan,*[a] Eric Pellegrin,*[c] Zhiwei Hu,[d] S. Manuel Valvidares,[c] Alessandro Barla,[ce] Wen-I. Liang,[f] Ying-Hao Chu,[f] Wenqin Zou[a] and Youwei Du[a]

Cooperation Nanjing University / MPI CPfS Dresden / CELLS-ALBA

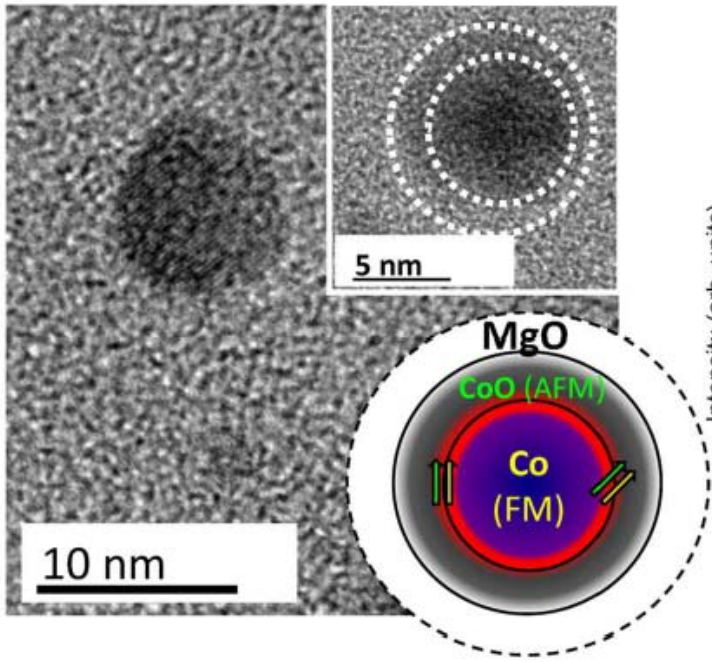

TEM pictures showing the size and morphology of the $Co_{69}Mg_7O_{24}$ sample, revealing the Co/CoO core–shell particles embedded in a MgO matrix.

Co2p XMCD on Co/CoO-MgO Core-Shell Systems

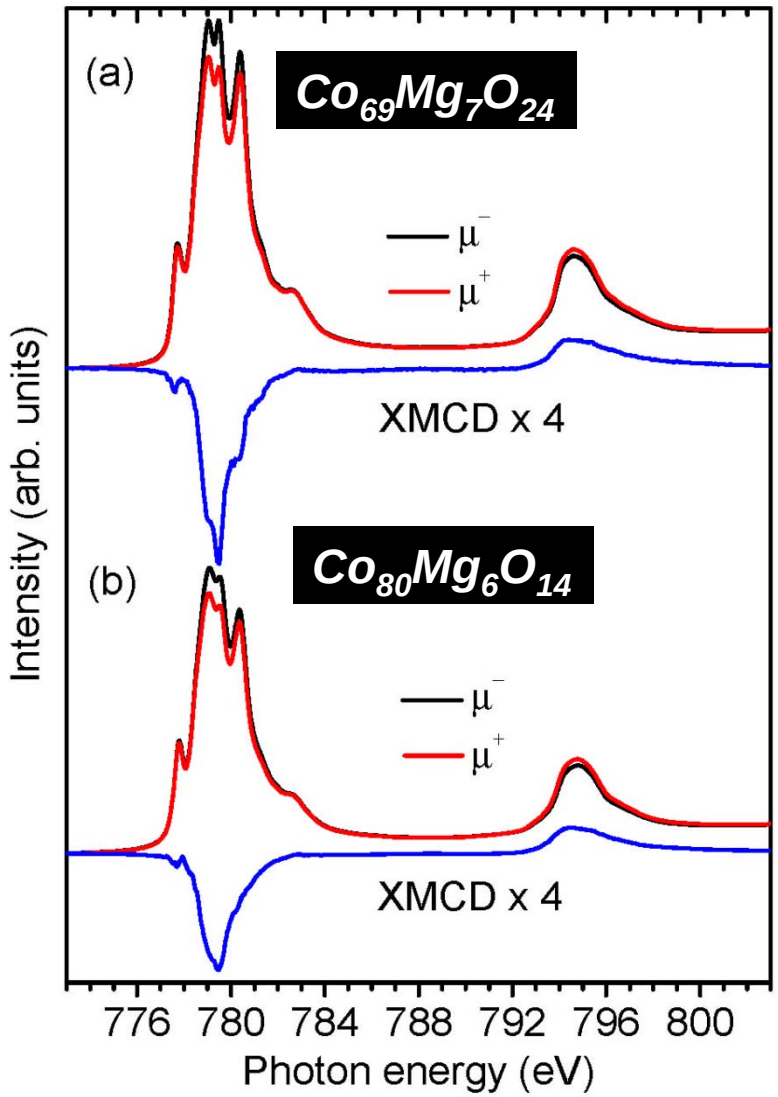

- **Co2p absorption spectra show typical line shape of Co^{2+}.**
- **Co2p dichroic spectrum shows multiplet structure typical for Co^{2+} in octahedral symmetry.**

Larger part of ferromagnetic signal stems from CoO shell.

Uncompensated rotatable Co^{2+} spins in nominally AFM CoO shell. Stabilized by MgO matrix.

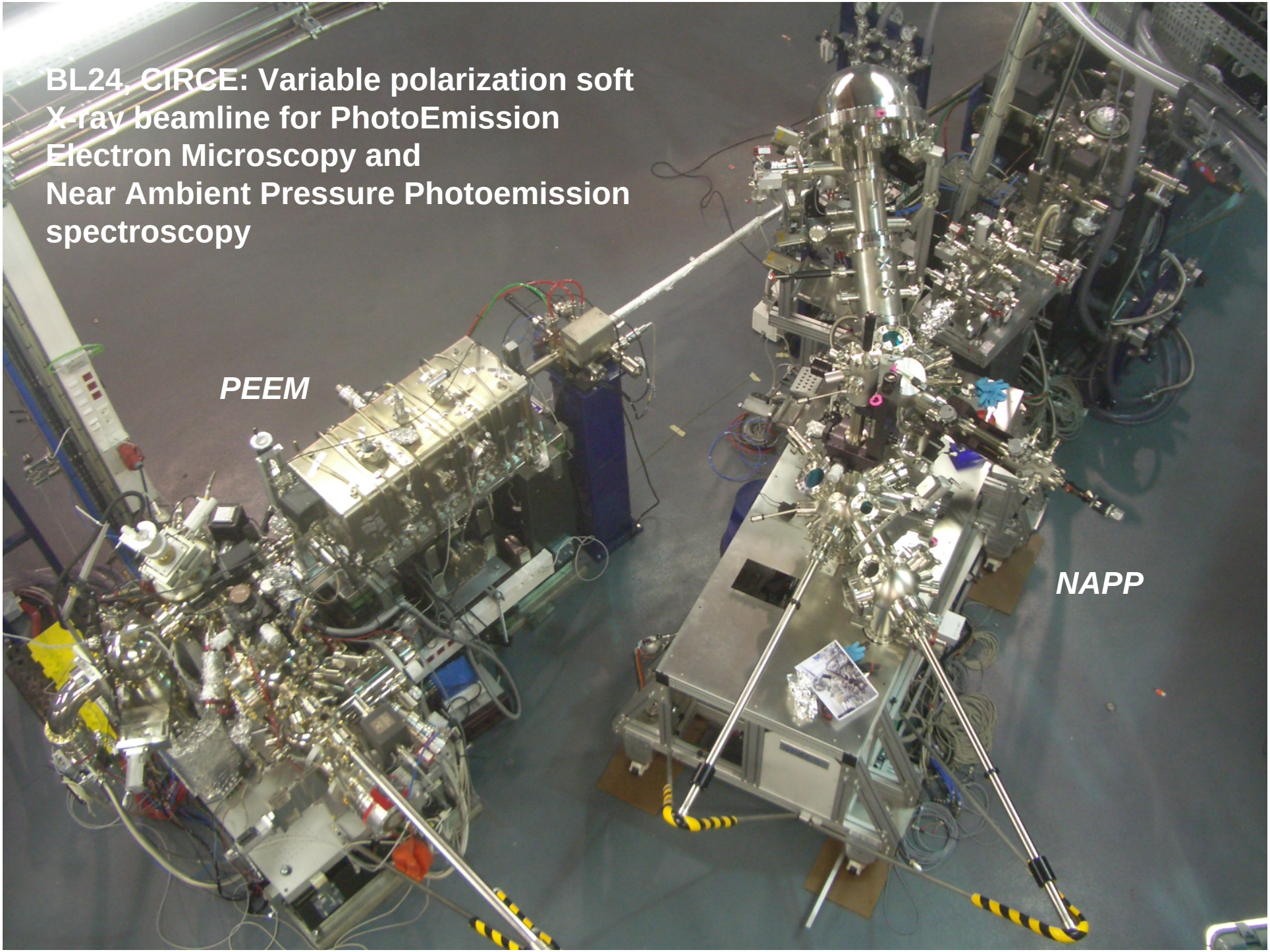
BL24, CIRCE: Variable polarization soft X-ray beamline for PhotoEmission Electron Microscopy and Near Ambient Pressure Photoemission spectroscopy
PEEM
NAPP

Photoemission Microscope (PEEM)

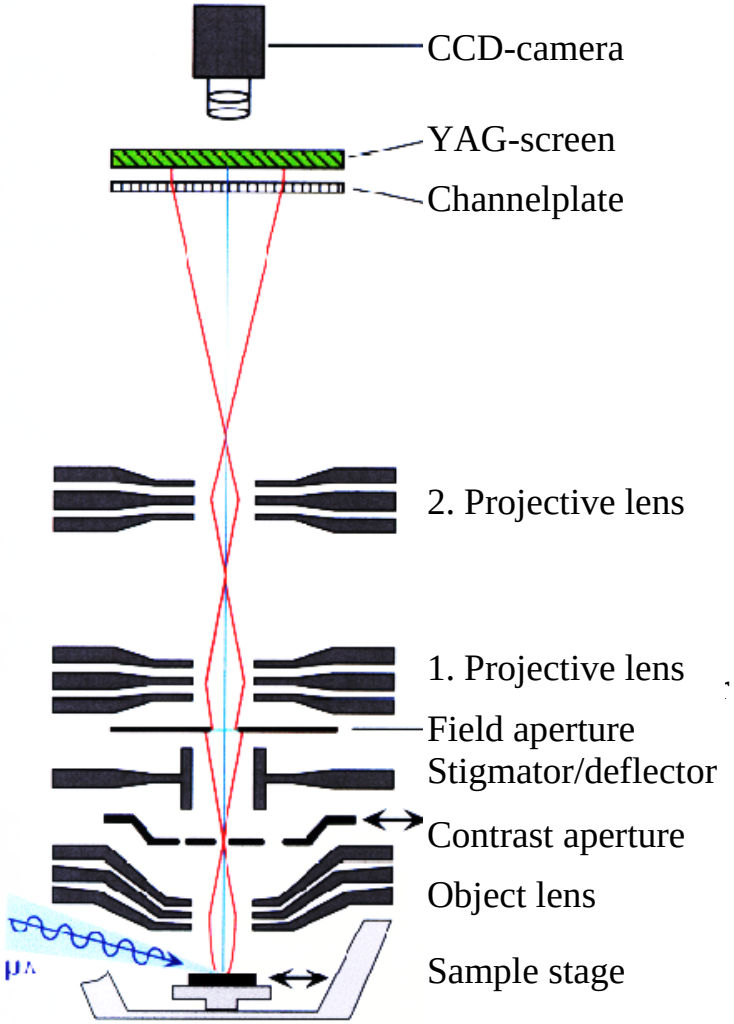

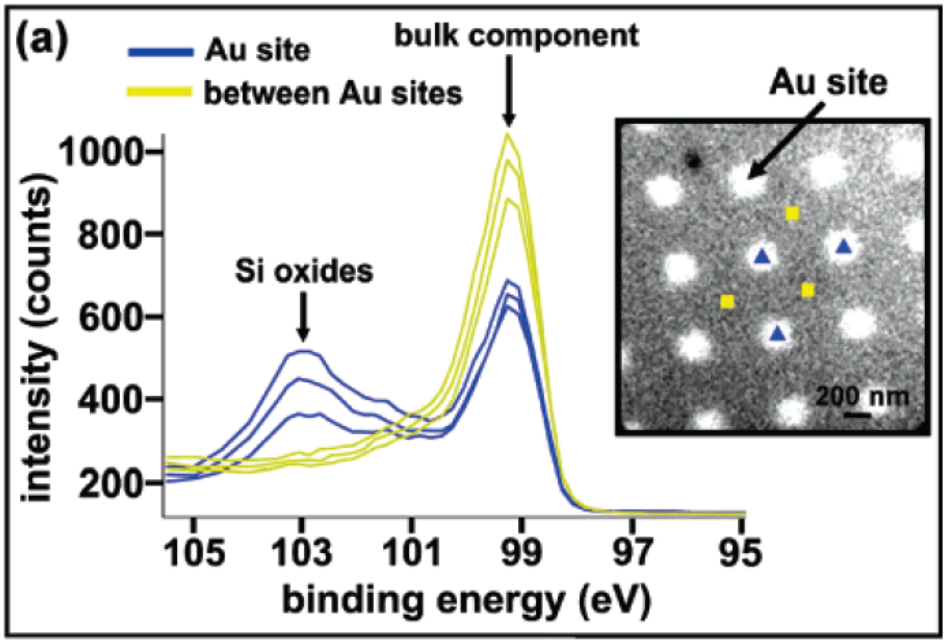

J. T. Robinson et al. Nanoletters vol 7 (2007)

Silicon is oxidized only at the Au sites

Phase Separation of Palmitic Acid and Perfluorooctadecanoic Acid in Mixed Langmuir−Blodgett Monolayer Films

Shatha E. Qaqish,[†] Stephen G. Urquhart,[†] Uday Lanke,[†] Sophie M. K. Brunet,[‡] and Matthew F. Paige*,[†]

Langmuir **2009,** *25(13),*

Two surfactants adsorbed on Si:

- HC : saturated hydrocarbed based; C1s → σ^*_{C-H} : 287.9 eV
- PF: perfluorocarbon C1s → σ^*_{C-F} : 292.8 eV

XPEEM reveals the phase separation of both species:

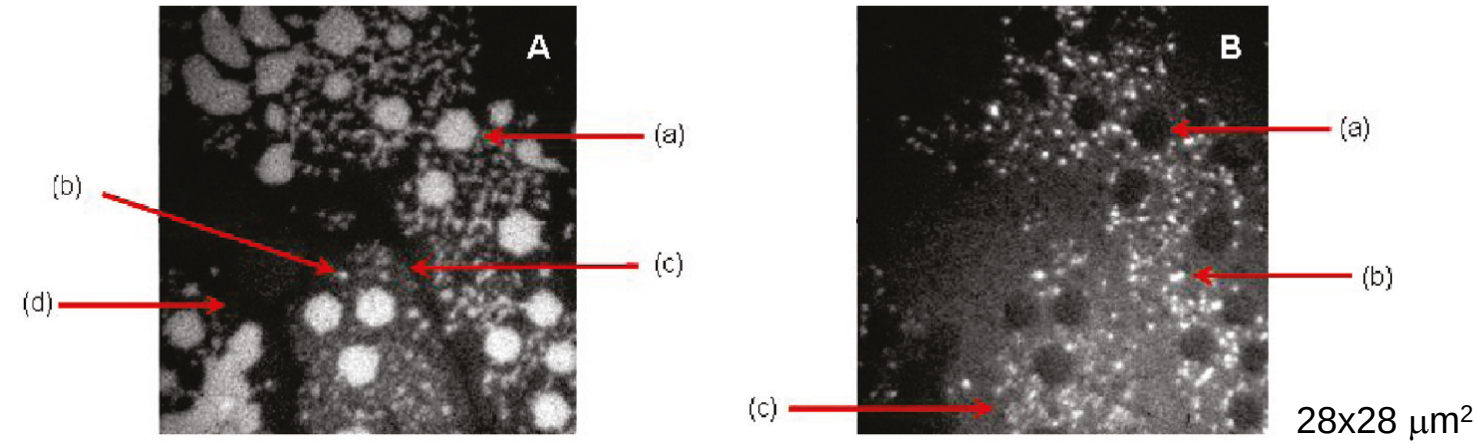

287.9 eV
HC sensitive

292.8 eV
PF sensitive

What is ARPES?

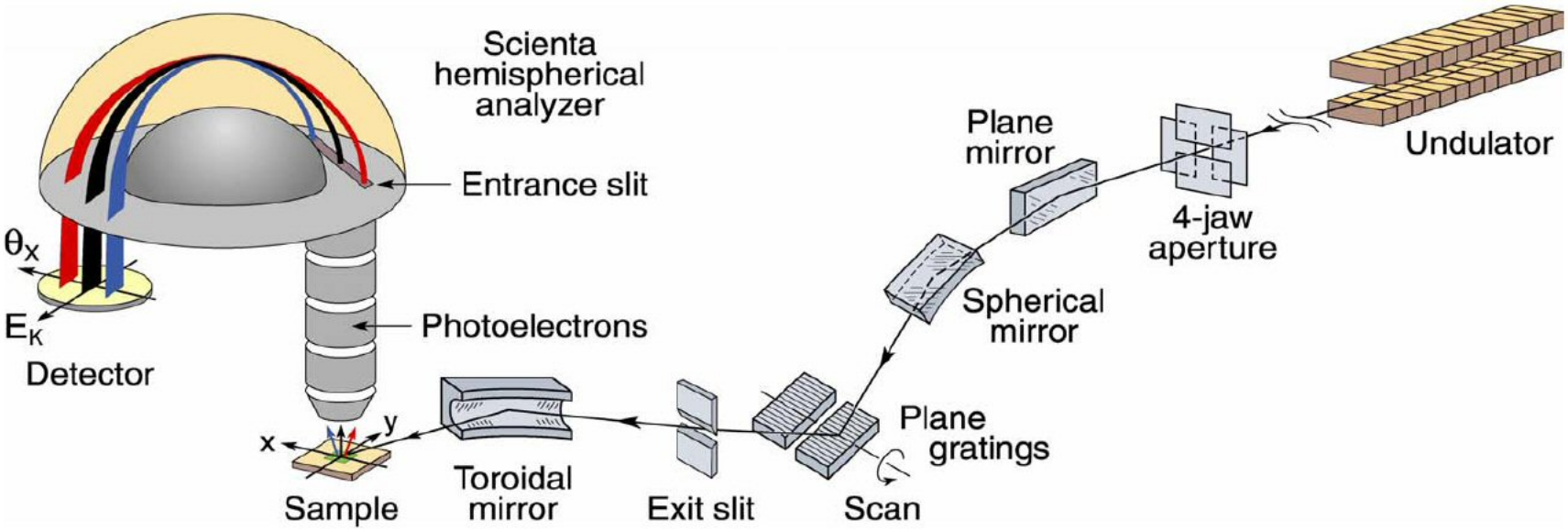

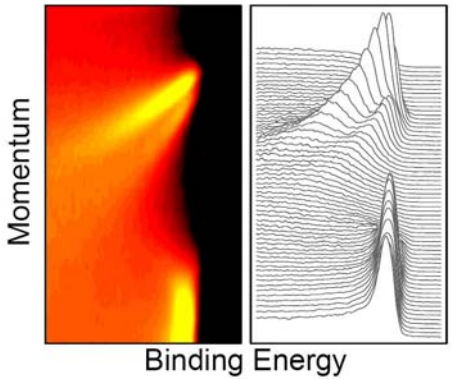

Direct mapping of the band structure

Direct *k* Space Imaging

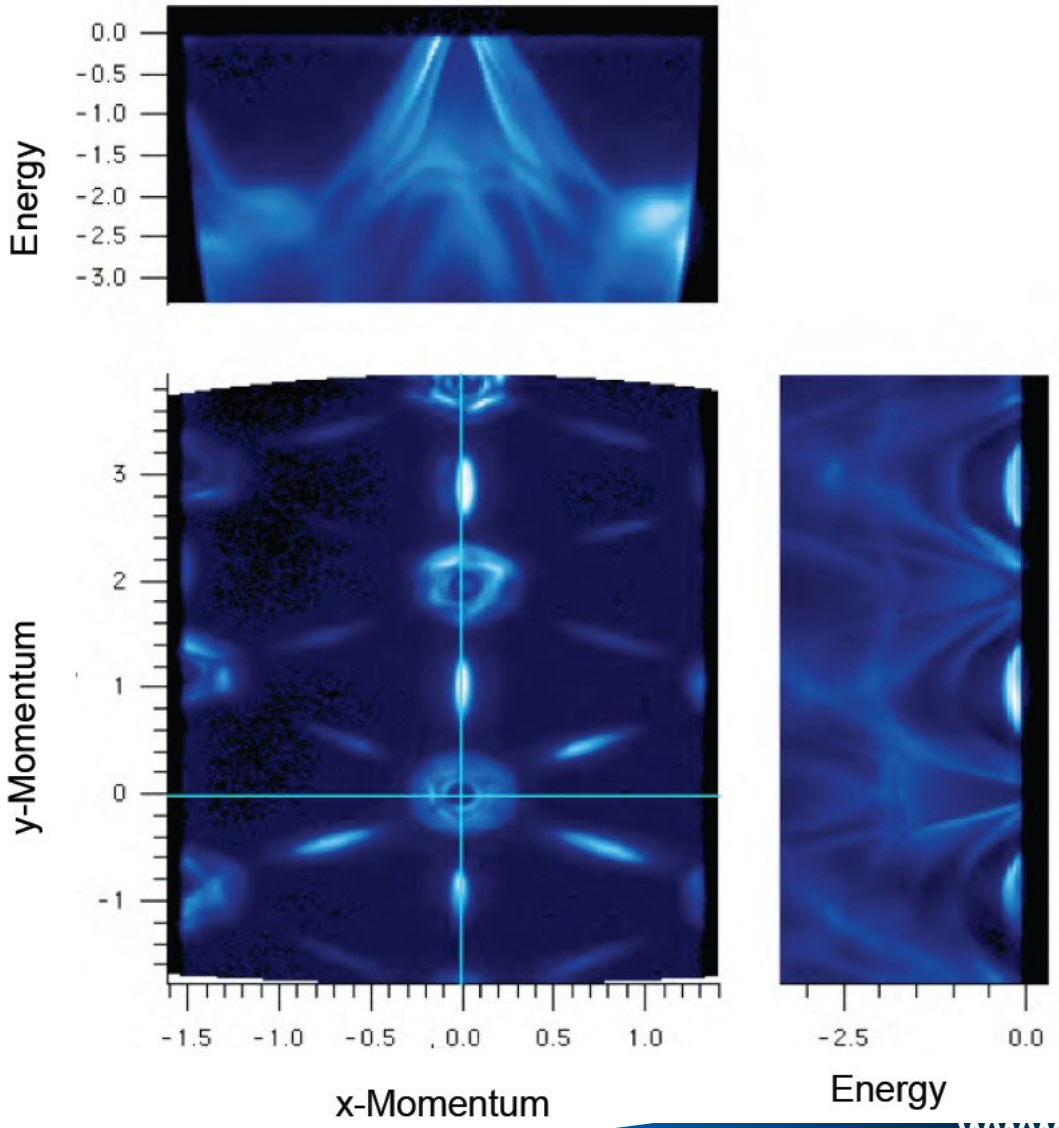

Infrared spectroscopy : light frequencies that coincide with vibrational modes of the sample are absorbed

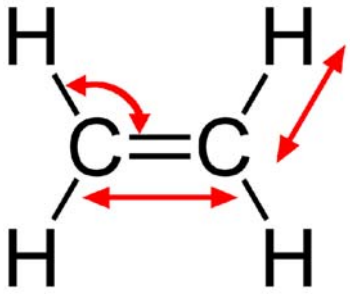

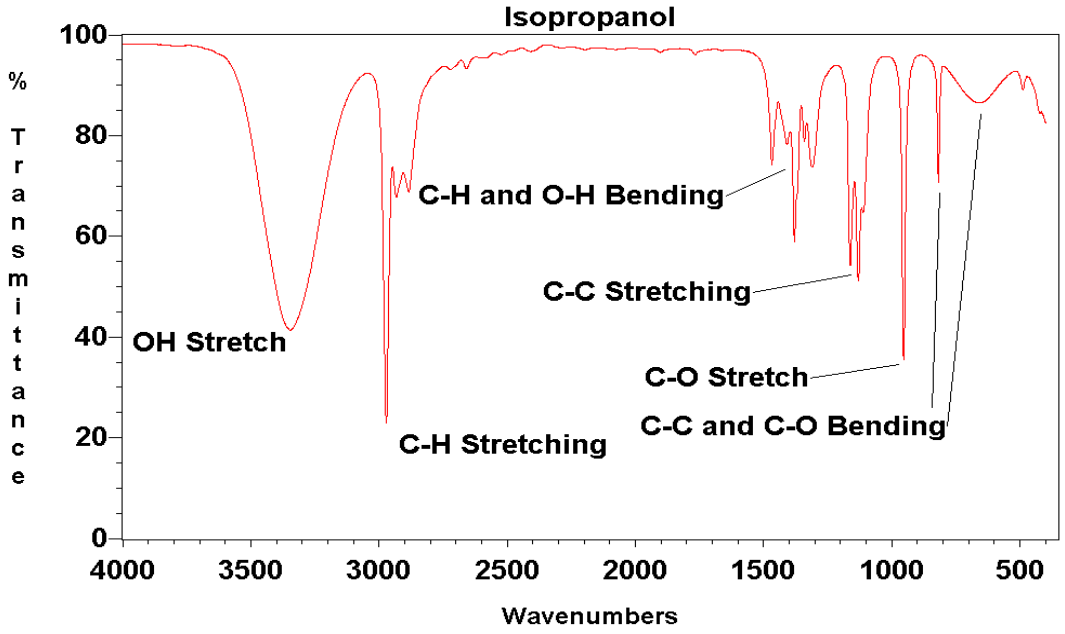

MIRAS: Spectro-imaging Infrared beamline

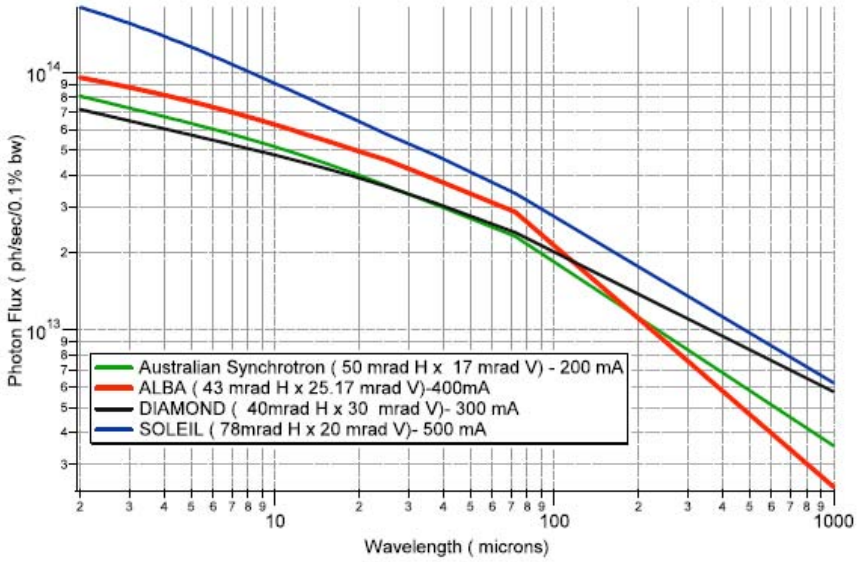

Fig. 4.2. Calculated flux at ALBA (red line), considering the proposed extraction of 45 mrad (H) x 25.17 mrad (V), and its comparison with SOLEIL (blue), DIAMOND (black), and Australian Synchrotron (green)

Bending magnet radiation
Microscopy resolution : 1 μm : low
BUT: live samples may be studied

Applications in: Material Science
Cultural Heritage
Medicine

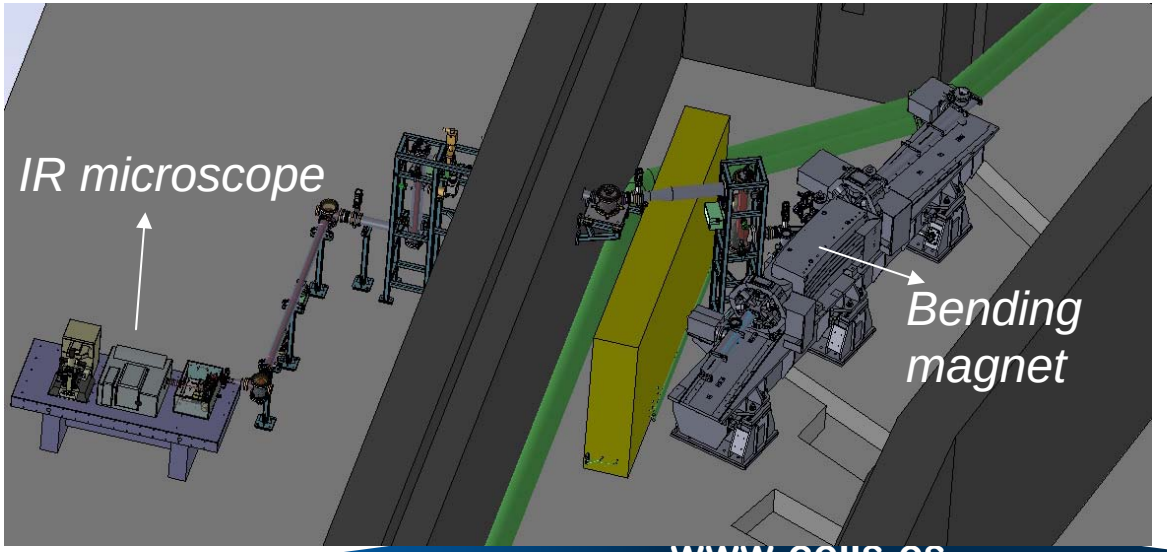

IR spectroscopy has a large variety of applications : textile

Raw cotton : hydrophobic. Treatments for removing waxes

A vibration at 1736 cm-1 is used as fingerprint

a: Raw cotton

b: After bio-treatment

c: After exposure to HCl vapor

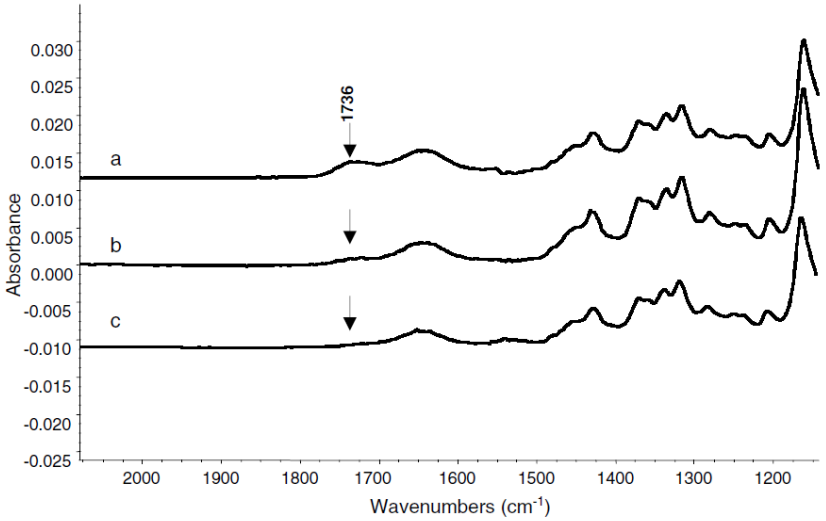

HCl vapor exposure treatments are energy consuming and pollutant. The authors show that bio-treatment (pectinase enzyme from Bacillus subtilis) is as efficient as HCl

Q. Wang et al. / Carbohydrate Research 341 (2006) 2170–2175

IR spectroscopy has a large variety of applications : wood

By analyzing in detail the IR spectra from cellulose in different woods, an IR characterization was achieved : IR allows quick evaluation of wood samples

A: Softwood: pine , spruce, *juniperus communis*

B: Hardwood: silver birch , birch ,lecus

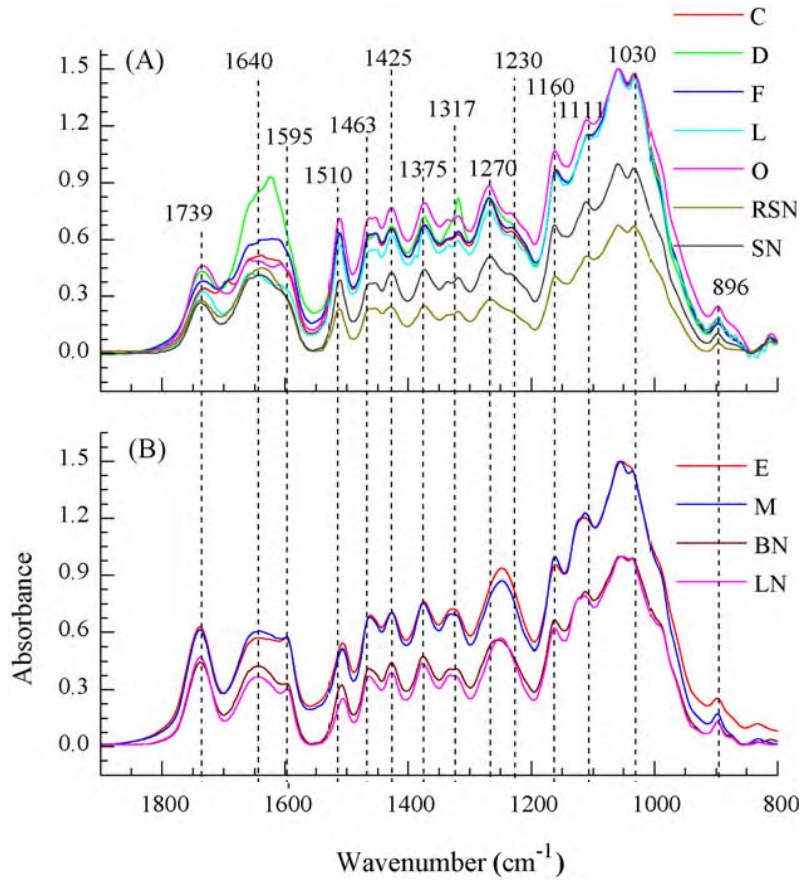

H. Chen et al. / Carbohydrate Polymers 82 (2010) 772–778

IR spectroscopy has a large variety of applications : pharmaceutical

Research on biodegradable PLGA (polyD,L- lactide-co-glycolide) coating for parenteral usage.

Lysozyme was inserted in PLGA matrix tablets and IR imaging was used to investigate the time-dependent spatial microenvironmental changes

4 days

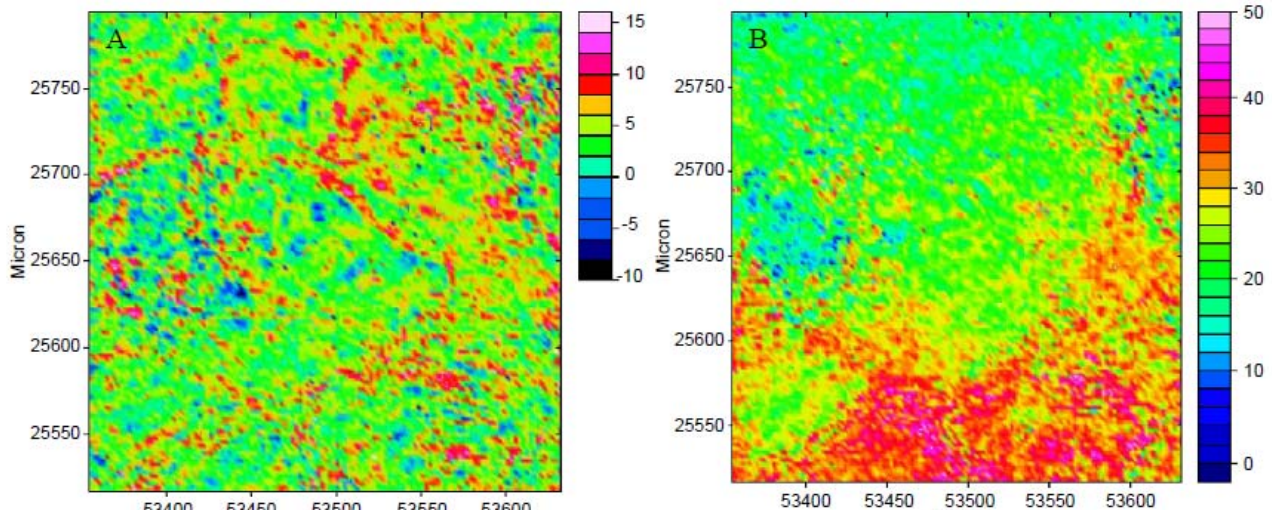

14 days

Fig. 8. False-color near-infrared images of lysozyme distribution (10% initial loading) at the surface of a poly(D,L-lactide-co-glycolide) tablet (A) after 4 days in PBS pH 7.4 and (B) after 14 days in PBS pH 7.4 (T=37 °C).

The images indicate that protein absorption on the PLGA matrix takes place

Possible phase III beamlines

1. **Microfocus diffraction beamline for macromolecular crystallography**
2. **Submicrometer-beam diffraction, fluorescence and absorption beamline**
3. **High-energy imaging and diffraction beamline**
4. **Surface-interface diffraction beamline**
5. **Energy and polarization dependent scattering beamline**
6. **Biomedical applications (imaging and therapy) beamline**
7. **Skiron: Chiroptical spectroscopy beamline**

Metabolism of an As-based drug against acute leukaemia
μ-XRF imaging and spectroscopy on patient's hair

μ-SXRF mapping of hair from patient treated As_2O_3 <1 μmol/l, section 20 μm thick

(*I.Nicolis, E.Curis, S.Bénazeth Lab. de Biomathématique, Université Paris V)*

μ-XANES

Beam size 1x3 μm, Energy step 0.5 eV

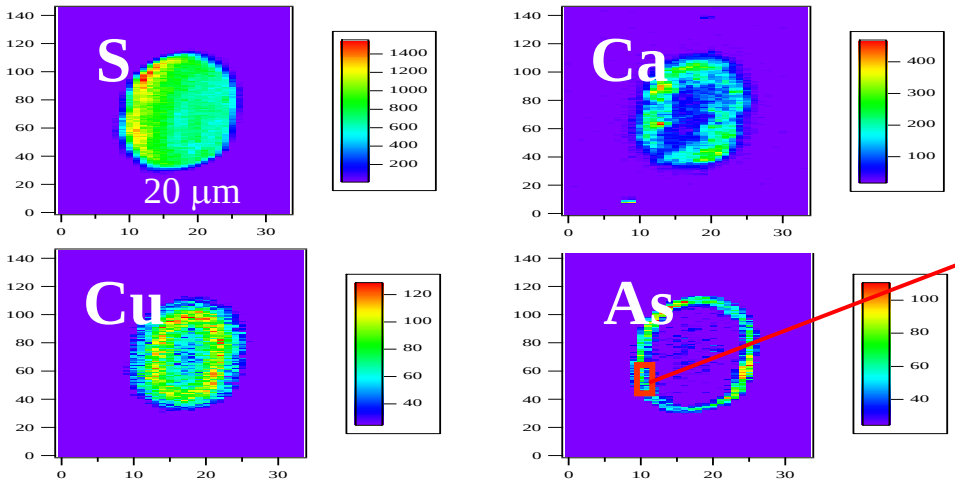

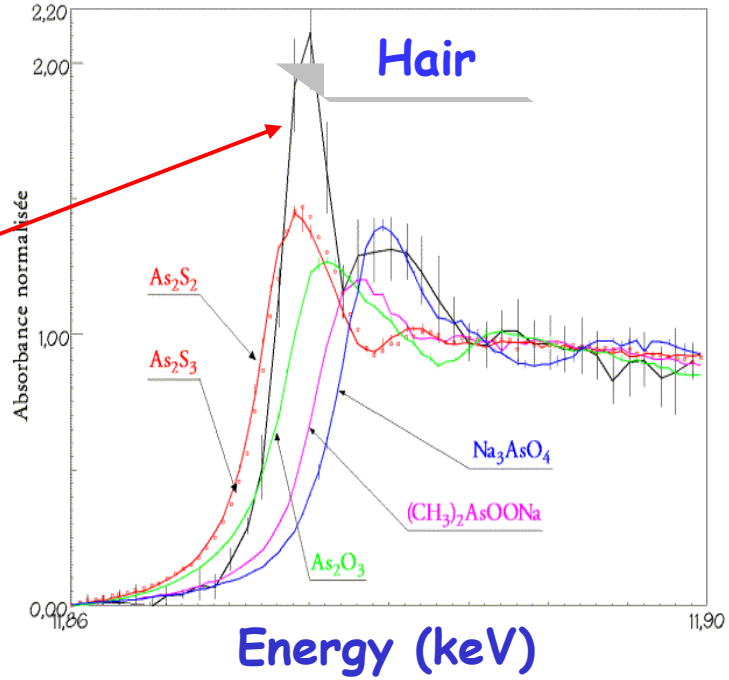

Phase III : tomographic imaging for material science

Imaging with high energy photons : microtomography

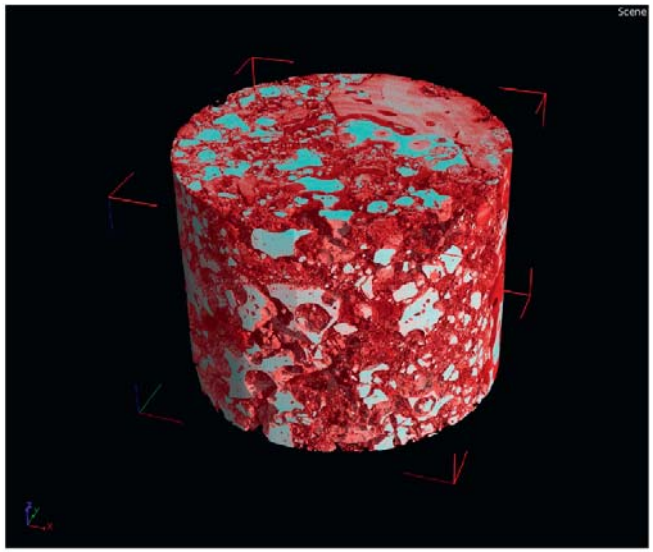

Human bone (red) with ceramic particles (white)

hv~35 keV

High resolution microtomography or computed tomography (CT) has become a routine tool for academia and industry alike for samples from all domains of science and sectors of industry. The CT reconstruction above shows a human regenerating-bone biopsy (red) with bioceramics particles (white) six months after implantation visualised using synchrotron-based high-resolution CT on ESRF beamline ID19. The diameter of the biopsy is 3mm.

Reference: M. Stiller, A. Rack, S. Zabler, J. Goebbels, O. Dalügge, S. Jonscher, C. Knabe
Quantification of bone tissue regeneration employing β-tricalcium phosphate by three-dimensional non-invasive synchrotron micro-tomography – a comparative examination with histomorphometry
BONE 44 (4), p. 619-628 (2009)
DOI 10.1016/j.bone.2008.10.049

Image courtesy of Alexander Rack, ESRF

Imaging with high energy photons : applications to metallurgy

Metallic glass foam yielding by percolation

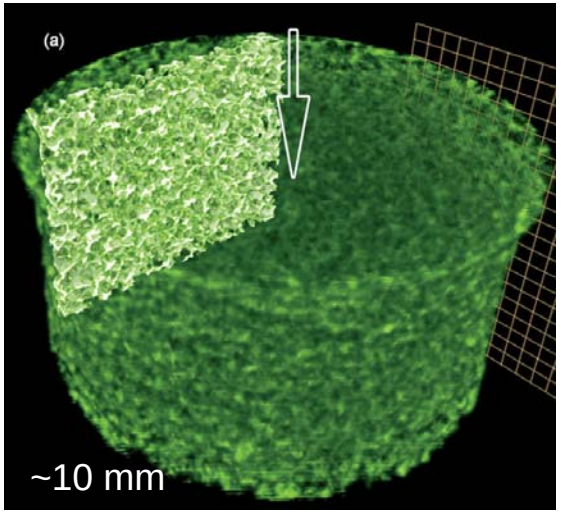

M. D. Demetriou et al.

Adv. Mater. **2007**, *19*, 1957–1962

ESRF hν ~50 keV

Al- 4%Cu alloy during solidification (-2˚C/min)

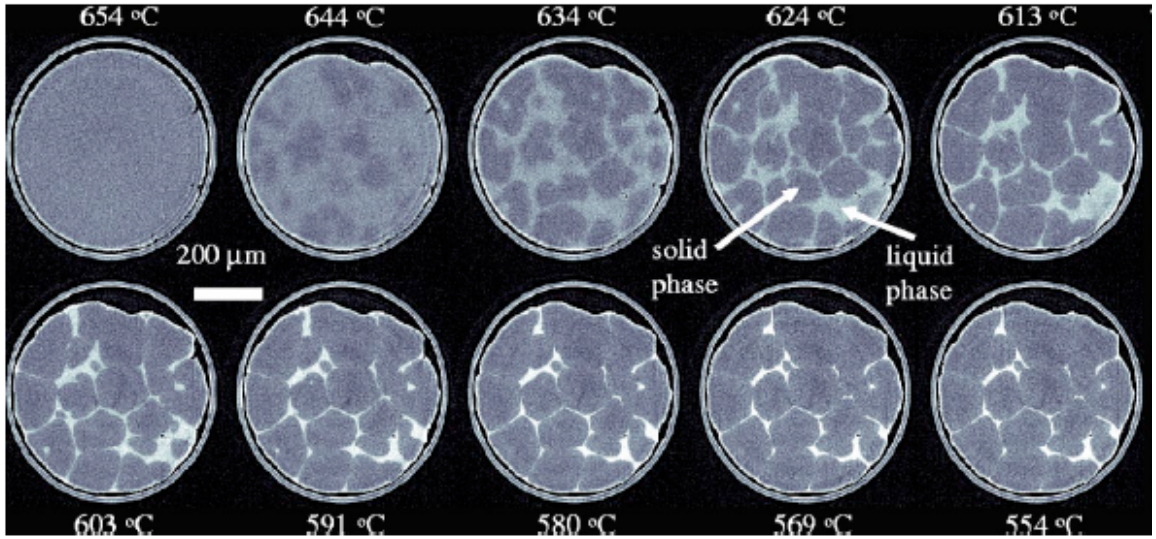

ESRF , hν = 44 keV

Liquid : Cu rich : high absorption
Solid : Cu poor : low absorption

M. Di Michiel et al.

REVIEW OF SCIENTIFIC INSTRUMENTS 76, 043702 (2005)